View metadata, citation and similar papers at core.ac.uk

brought to you by CORE

provided by Digital.CSIC

APPLIED PHYSICS LETTERS **104**, 172107 (2014)

Tensile strain mapping in flat germanium membranes

S. D. Rhead,[1,a)] J. E. Halpin,[1] V. A. Shah,[1,2] M. Myronov,[1] D. H. Patchett,[1] P. S. Allred,[1] V. Kachkanov,[3] I. P. Dolbnya,[3] J. S. Reparaz,[4] N. R. Wilson,[1] C. M. Sotomayor Torres,[4,5] and D. R. Leadley[1]

[1]*Department of Physics, University of Warwick, Coventry, CV4 7AL, United Kingdom*
[2]*Department of Engineering, University of Warwick, Coventry, CV4 7AL, United Kingdom*
[3]*Diamond Light Source, Harwell Science and Innovation Campus, Didcot, Oxfordshire, OX11 0DE, United Kingdom*
[4]*ICN2 - Institut Catala de Nanociencia i Nanotecnologia, Campus UAB, 08193 Bellaterra (Barcelona), Spain*
[5]*ICREA, Passeig Llu´s Companys 23, 08010 Barcelona, Spain*

(Received 13 January 2014; accepted 18 April 2014; published online 2 May 2014)

Scanning X-ray micro-diffraction has been used as a non-destructive probe of the local crystalline quality of a thin suspended germanium (Ge) membrane. A series of reciprocal space maps were obtained with ~4 μm spatial resolution, from which detailed information on the strain distribution, thickness, and crystalline tilt of the membrane was obtained. We are able to detect a systematic strain variation across the membranes, but show that this is negligible in the context of using the membranes as platforms for further growth. In addition, we show evidence that the interface and surface quality is improved by suspending the Ge. © *2014 AIP Publishing LLC*. [http://dx.doi.org/10.1063/1.4874836]

Germanium (Ge) is a logical supplement to enhance existing silicon (Si) semiconductor technologies, as its material behavior is very similar to Si, and it allows new and improved functionality.[1] Ge has potential in spintronic,[2] optical detection,[3] and lasing[4] fields and is an accommodating buffer for III-V materials making it an excellent platform for photonic devices.[5,6] Major advantages of growing Ge epitaxially on Si are that Ge based devices can be manufactured on a Si substrate, using existing Si technologies, and that the Si (001) substrate has superior mechanical properties compared to bulk Ge (001): it is lighter, less brittle, and considerably less expensive to produce. However, due to the large 4.2% lattice mismatch between Ge and Si only a few monolayers of Ge can be grown pseudomorphically on Si (001), with thicker layers relaxing to the bulk Ge lattice parameter through the formation of misfit and threading dislocations. Nevertheless, high-quality crystalline Ge layers can be grown epitaxially on Si (001) that are almost fully relaxed, with sub-nm roughness and low defect densities,[7–9] although such epitaxial Ge on Si is still susceptible to electrical leakage by conduction through the dislocation network still present in the layer.[10–12] Generally, research efforts have focused on reducing the threading dislocation density (TDD); however, it has been speculated that the deleterious surface-to-surface conduction could be prevented if instead the misfit dislocations could be removed.[13] A possible approach to achieve this is by suspending the Ge layer, which would remove the Ge/Si interface and potentially the majority of the misfit dislocation network. In this way, tensile strained Ge membranes could be enabled for use as platforms for complimentary metal-oxide-semiconductor (CMOS), optoelectronic and cryogenic integration purposes.

Ge membranes, that remain atomically flat by being suspended under tensile strain, also offer a crystalline alternative to other popular membrane materials such as silicon nitride (Si_3N_4). In the case of Si_3N_4, strain can be controlled using plasma enhanced chemical vapor deposition growth techniques; however, it is an amorphous insulator which limits further epitaxial growth of semiconductor materials and the fabrication of solid state devices directly onto its surface. Most integrated circuitry is fabricated on single crystal substrates, due to the enhancements in charge carrier lifetime[14] and its mobility[15] within the material, as well as a higher yield of functional devices than from polycrystalline material where inconsistencies arise due to small differences in grain size.[16] Single crystal material also has good thermal transport properties compared to poly-crystalline and amorphous materials.[17] This is important for room-temperature microelectromechanical systems (MEMS) devices, such as accelerometers, gyroscopes, and micro-mirror devices[18] that are found in today's smartphones. In the particular case of micro-mirrors, an essential component in a pico-projector system,[19] the surfaces need to be atomically smooth to increase the reflectance of visible light.[20] The need for flat MEMS surfaces is also required for other applications if integration of planar CMOS technology is to be incorporated on membrane-type platforms.[21] This could potentially allow Ge membranes to integrate optical technologies alongside CMOS and MEMS to be an all-round integration platform.

Realizing a Ge light source remains a particularly challenging goal, due to Ge being an indirect bandgap material. However, under sufficient tensile strain Ge can becoming a direct band gap material and so a tensile-strained Ge crystalline membrane could be a useful platform for a Ge light source, or other Ge-based optical devices. Recently, thin (<1 μm) freestanding Ge membranes[22,23] and various other suspended structures[13] have been fabricated through relatively simple processing. Nam *et al.*[22] and Kurdi *et al.*[24] have used such structures to show the electroluminescence and photoluminescence effect of further tensile straining a Ge membrane, but neither comment on the strain distribution across the membrane prior to strain. If the starting membrane

[a)]S.Rhead@warwick.ac.uk

 © 2014 AIP Publishing LLC

This article is copyrighted as indicated in the article. Reuse of AIP content is subject to the terms at: http://scitation.aip.org/termsconditions. Downloaded to IP: 161.111.180.191 On: Wed, 23 Dec 2015 11:22:53

is not homogenous in its properties then other effects apparently observed on further straining may be a composite from a spectrum of different strain values and in actuality luminescence may be shaper, rather than broader, in response to strain.[24] However, standard structural characterization such as transmission electron microscopy (TEM) and scanning probe microscopy of these membranes are difficult due to their fragility. Two dimensional strain maps can be determined indirectly using micro Raman spectroscopy[25] and spectroscopic ellipsometry;[26] however, analysis often requires prior knowledge of the structures and complex simulation of the data.

High-resolution X-ray diffraction (HR-XRD) is the non-destructive technique of choice for determining the composition, strain-relaxation and thickness of single-crystal materials. These parameters can be easily obtained once a Bragg reflection with a strong structure factor has been measured (such as the Si (004) Bragg Peak) and used as a reference point for all further data. However, for a standard lab-based diffractometer, the X-ray beam is typically several hundreds of microns in diameter, meaning that the measured HR-XRD is insensitive to localized, real-space changes of the composition or strain. In the past decade, significant progress has been made in the focusing of X-rays and spot sizes smaller than 100 nm are now achievable.[27] This allows a small X-ray beam to be scanned across a sample as a local probe in a similar fashion to scanning microscopy techniques. Consequently, micro- and nano-diffraction experiments have been used to determine the strain and composition of single micron sized SiGe islands,[28,29] strain relief in single patterned SiGe nanostructures,[30] silicon-on-insulator deformation induced by stressed linear structures,[31] and even the strain of a single SiGe quantum dot inside a field-effect transistor.[32] Etzelstorfer *et al*. have recently described the X-ray micro-diffraction of a suspended Ge bridge and the technique required, but the reported sample was one dimensional, so strain is uniaxial; the bridge was also thick (∼2 μm) and cracked, all of which points to a non-uniform strain distribution in the bridge.[33] In this study, we have used X-ray micro-diffraction to determine the local crystalline quality of a <150 nm thick suspended Ge membrane, for the purposes of evaluating its potential as a uniform platform on which further epitaxial heterostructures can be grown. The root mean square (RMS) roughness of the layers was determined using atomic force microscopy (AFM). An Asylum Research MFP-3D used in tapping mode was used with Si_3N_4 tips to capture the images. Plan-view transmission electron microscopy (PV-TEM) measurements were performed using a JEOL JEM-2000FX TEM operating at 200kV. No mechanical preparation of the samples was required as the membranes were thin enough to be electron transparent. A micro-Raman line scan across the membrane was measured as a comparison with the X-ray micro-diffraction. The Raman spectra were measured at room temperature with a high resolution HORIBA Jobin-Yvon spectrometer, using the 488 nm line of a mixed Ar:Kr laser in conjunction with a 50× objective. The focus diameter was approximately 1.2 μm. The Raman spectra were fitted using Lorentzian functions with a spectral accuracy of 0.03 cm^{-1}.

Ge layers were epitaxially grown on both sides of a double-sided polished Si (001) substrate by reduced-pressure

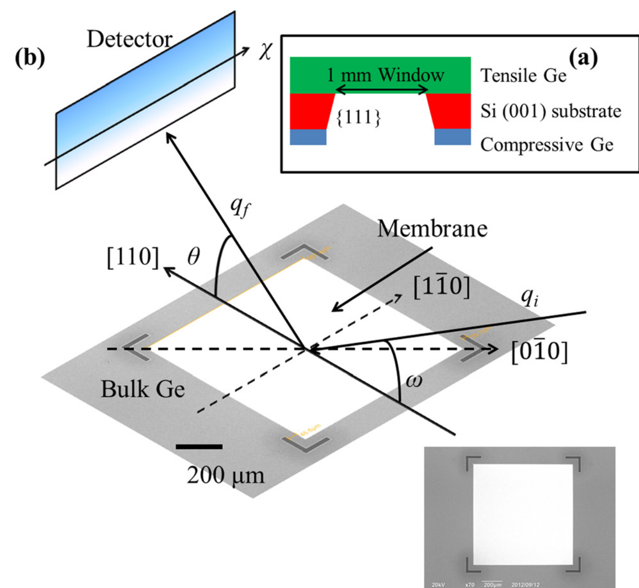

FIG. 1. (a) Schematic of the suspended Ge membrane. (b) A scanning electron microscope (SEM) image of the suspended Ge membrane with the (004) scattering geometry overlaid. The membrane edges are aligned parallel to the ⟨110⟩ directions. RSMs at each spatial point are obtained by scanning along the [1$\bar{1}$0] and [0$\bar{1}$0] directions. The plan view SEM image is shown in the bottom right. The bulk Ge is dark grey whilst the membrane is bright white.

chemical vapor deposition in an ASM Epsilon 2000 system using a germane precursor.[7] Prior to fabrication, the top-side Ge layer was 200 nm thick and under slight tensile strain, which arises during the epitaxial growth of Ge on Si; although the Ge layer is fully relaxed at growth temperatures it becomes tensile strained during cooling due to the difference in thermal expansion of the Ge and Si. The Ge membrane is fabricated in several stages.[13] The ∼1 × 1 mm window, over which the Ge membrane was suspended, was first defined by optical lithography and reactive ion-etching on the bottom-side Ge layer. Then, the sample was etched in a 25% wt. tetramethylammonium hydroxide (TMAH) bath at 85 °C for approximately 12 h. The TMAH selectively etches the {001} Si planes whereas the {111} planes are etch resistant.[34] Ge is extremely etch-resistant to TMAH and as a result the top-side Ge is suspended over a 1 mm^2 window (Fig. 1(a)). The Ge membrane is slightly thinned after etching to a thickness of 80-120 nm, but remains under tensile strain as it is fixed to the Ge-on-Si (001) frame.

Micro-diffraction experiments were performed on beamline B16 at the DIAMOND Light Source[35] using X-rays with an energy of 12.4 keV (wavelength = 1 Å). A compound refractive lens was used to focus the X-ray beam with a spot size of 3.72 μm × 1.85 μm (horizontal × vertical). Due to the angle of incidence the beam footprint was approximately circular with a diameter of ∼4 μm. The sample was mounted on a *XYZ* stage (with 0.5 μm precision) in a five circle diffractometer allowing the sample to be moved through the beam (Fig. 1(b)). Local heating caused by the beam has the potential to either damage the structures or distort strain results by thermal expansion; therefore to mitigate these effects the sample was actively cooled by a nitrogen jet at low flow at 20 °C. Scattered X-rays were collected by a large PILATUS 300 K area detector. To locate the membrane, the

This article is copyrighted as indicated in the article. Reuse of AIP content is subject to the terms at: http://scitation.aip.org/termsconditions. Downloaded to IP: 161.111.180.191 On: Wed, 23 Dec 2015 11:22:53

diffractometer was aligned to the Si substrate (004) peak and the disappearance of this peak was observed as the sample was moved to a position where the beam only impinges on the suspended membrane without its Si substrate. The diffractometer was then aligned onto the Ge (004) peak on the bulk frame of the membrane and the detector centered on a scattering angle (2θ) halfway between the Si substrate and Ge layer peaks. Reciprocal space maps (RSMs) as a function of position where obtained by rotating ω around the (004) reflection at each spatial point and rastering the sample through the beam.

The strain along the membrane was characterized by measuring (004) RSMs every 10 μm along the $[1\bar{1}0]$ direction across the middle of the sample (Fig. 1(b)). The membrane edge, incident and scattered X-rays were all parallel to the [110] direction of the crystal and the spatial resolution of the RSMs given by the spot size ($\sim$4 μm). The RSMs obtained for selected positions along the sample are shown in Fig. 2. An RSM containing both the Si substrate and Ge (004) peaks is shown in Fig. 2(a). The Si substrate peak is fixed at $q_{\parallel} = 0 \pm 0.00003$ Å^{-1} (the parallel scattering component) and $q_{\perp} = 0.7365 \pm 0.00003$ Å^{-1} (the perpendicular scattering component) and is used as a reference throughout. The Ge peak is centered on $q_{\parallel} = 0 \pm 0.00003$ Å^{-1} for both the supported and suspended Ge (Figs. 2(a) and 2(c)), confirming the absence of tilt in the lattice plane in these regions, whereas there is a significant peak shift at the membrane edge (Fig. 2(b)) that is most likely due to bending of the lattice planes as a result of partial strain relaxation in this transition region. Diffraction profiles as a function of $q_{\perp}$ (with $q_{\parallel} = 0$ Å^{-1}) for the supported Ge and the middle of the Ge membrane are shown in Fig. 2(d). There is a slight peak shift to higher $q_{\perp}$ at the middle of the membrane corresponding to a decrease in the out-of-plane Ge lattice parameter ($a_{\perp}$). The reduction in intensity is simply a result of the bulk material being slightly thicker than the membrane. Pendellösung ("thickness") fringes are observed in the membrane profile (the separation of the fringes corresponds to a membrane thickness of 114 $\pm$ 5 nm), but not for the supported Ge profile. These fringes arise from interference of X-rays reflected from the top and bottom of thin films and are often not visible due to lateral sample inhomogeneities. For the supported Ge there are misfit dislocations at the substrate-layer interface, resulting from the 4.2% lattice mismatch between Si and Ge. The region close to the defects will be strained and distorted, which will disrupt the X-ray wavefields in the region of the interface and causes the X-rays reflected from the surface and interface to become incoherent; as a result the thickness fringes disappear.[36] The observation of thickness fringes on the membrane suggests that the misfit dislocation network is removed along with the Si substrate and confirms that the membrane is uniform along $[1\bar{1}0]$. A line scan along the $[0\bar{1}0]$ direction from corner to corner (not presented here) was obtained by rotating the sample by 45° and displayed identical behavior to the line scan along the middle of the membrane. This result confirms the membrane surface is uniform across the entire membrane.

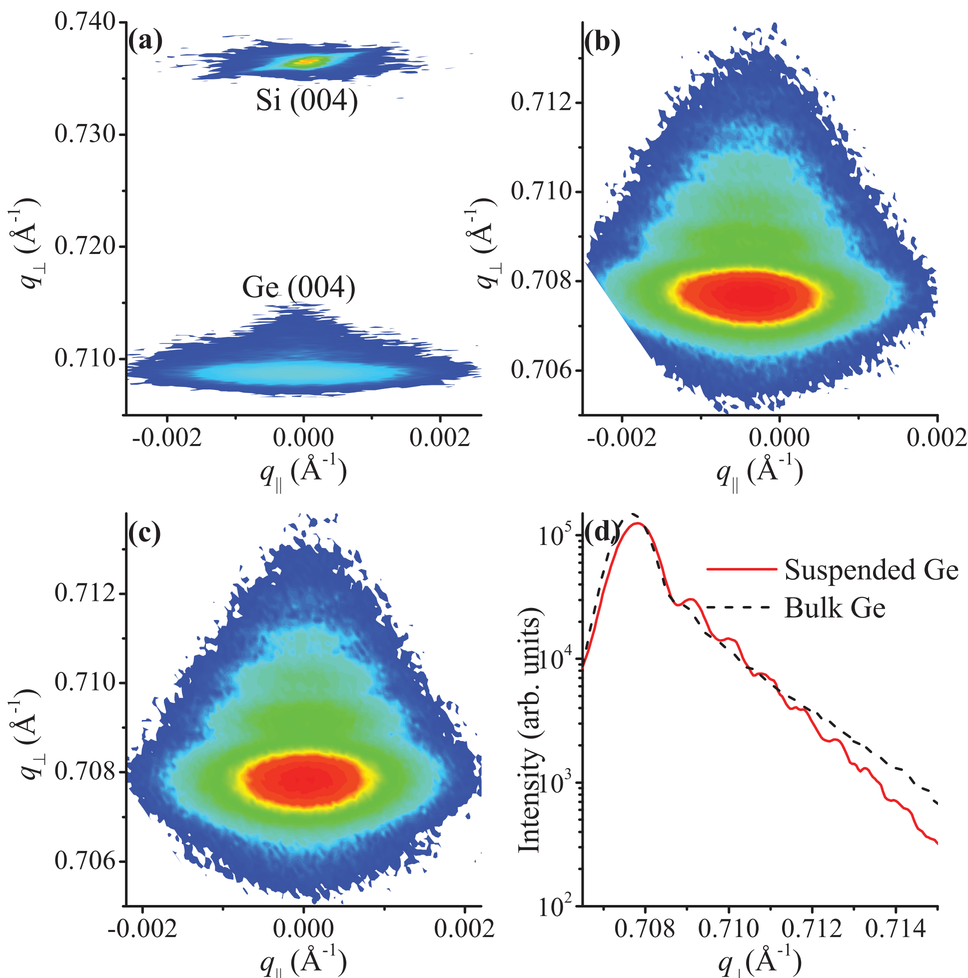

FIG. 2. (004) RSMs from various regions of the sample; (a) Ge on the Si substrate, (b) the membrane edge and (c) the middle of the Ge membrane. (d) Line profile extracted from the RSMs.

This article is copyrighted as indicated in the article. Reuse of AIP content is subject to the terms at: http://scitation.aip.org/termsconditions. Downloaded to IP: 161.111.180.191 On: Wed, 23 Dec 2015 11:22:53

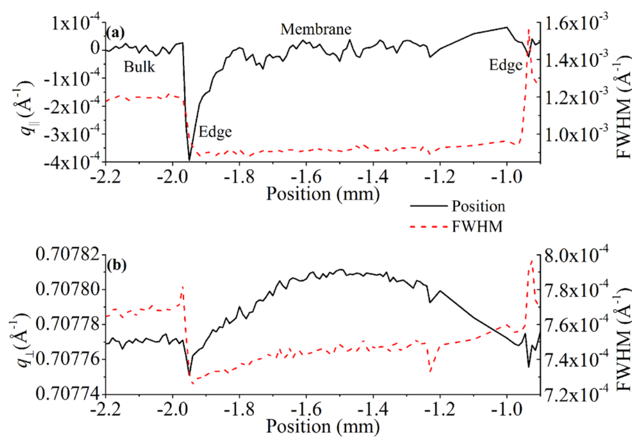

FIG. 3. Position and FWHM of the (004) Ge Bragg peak as a function of position for (a) $q_{\parallel}$ and (b) $q_{\perp}$.

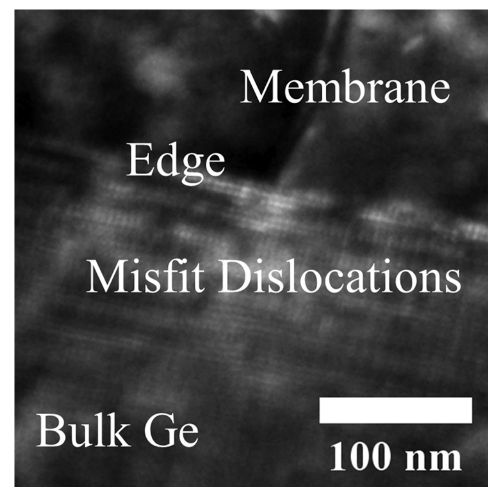

FIG. 4. PV-TEM micrograph of the membrane edge.

The Ge peak position and full-width half maximum (FWHM) as a function of real space position are shown in Figure 3. The FWHM of the Ge peak for both $q_{\perp}$ and $q_{\parallel}$ is widest for the supported material and narrowest on the membrane. The broadened peak in $q_{\parallel}$ (i.e., along [110]) from the supported Ge is a result of diffuse scattering that arises from the misfit dislocation network. The peak is centered on $q_{\parallel} = 0 \pm 0.00003$ Å^{-1} along the supported Ge, but suddenly drops to $q_{\parallel} = -0.0004 \pm 0.00003$ Å^{-1} at the left membrane edge (corresponding to a crystal tilt of $\sim$0.035°) before returning to 0 Å^{-1} across the remainder of the membrane. The edge effect is less pronounced at the right hand side because the sample was not mounted exactly flat on the sample stage but was slightly raised on the right edge compared to the left edge (seen as the slight drift in the FWHM). This result confirms that, apart from at its edges, the membrane itself is free from tilt and is flat relative to the original Si wafer. In the perpendicular direction, the Ge peak from the supported region is found at approximately $q_{\perp} = 0.70777 \pm 0.00003$ Å^{-1} ($a_{\perp} = 5.6516 \pm 0.0003$ Å) and there is a sudden drop to $q_{\perp} = 0.70775 \pm 0.00003$ Å^{-1} ($a_{\perp} = 5.6517 \pm 0.0003$ Å) at the membrane edge. As the epitaxial Ge layer is under tensile strain the peak shift to lower values confirms partial strain relaxation at the membrane edge leading to bending of the lattice planes. There is a gradual increase in $q_{\perp}$ from the edge to the middle of the membrane where $q_{\perp} = 0.70781 \pm 0.00003$ Å^{-1} ($a_{\perp} = 5.6512 \pm 0.0003$ Å) and then a subsequent decrease approaching the edges. Assuming the pure Ge behaves elastically, strain relaxation can be calculated easily. The bulk material is 103.72% relaxed (confirmed by lab based XRD) and the membrane edge and middle are 103.64% and 103.91% relaxed, respectively. The in-plane strain ($\varepsilon_{\parallel}$) is 1.55×10^{-3}, 1.51×10^{-3} and 1.63^{-3} on the bulk, edge and middle of the membrane and demonstrates the strain profile is symmetrical across the middle of the membrane and the membrane is slightly more tensile strained than the supported Ge. The $[0\bar{1}0]$ line profiles again show identical behavior to the $[1\bar{1}0]$ demonstrating uniformity across the membrane.

A typical PV-TEM micrograph of the bulk, edge and membrane is displayed in Fig. 4 and the TDD is approximately 3×10^{9} cm^{-2} for the bulk and suspended Ge, however, whereas a misfit dislocation network is observed at the Si/Ge interface this network disappears when the Si substrate is removed. The surface morphology across the membrane edge measured by AFM is shown in Fig. 5(a). A line profile across the membrane edge is extracted from this scan (Fig. 5(b)). The height range is approximately 2 nm on the bulk and membrane. The bulk and membrane are averaged on 0 nm but there is a drop at the edge to ~ -2.5 nm. This recovers to 0 nm 45-50 μm away from the membrane edge; explaining the large tilt at the edge shown by the X-ray line profile. A line profile across the middle of the membrane (not presented here) shows the membrane is flat with a height range of $\sim$2 nm. The surface of the suspended material is also smoother than the bulk material; the RMS roughness of the membrane is 2.16 ± 0.16 nm whereas the RMS roughness of the bulk material is 2.66 ± 0.05 nm. This shows that by suspending the Ge membrane both the interface and surface quality are improved.

A micro-Raman line scan across the middle of the membrane was performed in a similar manner to the scanning X-ray micro-diffraction. Raman spectra were measured every 10 μm and the peak position of the GeGe optical phonon tracked. The phonon frequency was found at $\sim$300 cm^{-1} and $\sim$299.5 cm^{-1} for the supported and suspended Ge, respectively, corresponding to a $\varepsilon_{\parallel}$ of $\sim 1.4 \times 10^{-3}$ and $\sim 1.55 \times 10^{-3}$, respectively.[37] There is relatively good agreement between the two techniques and in both methods the membrane is more tensile strained than the bulk material and symmetric across the membrane. However, the resolution of $\varepsilon_{\parallel}$ is significantly poorer when measured with Raman and

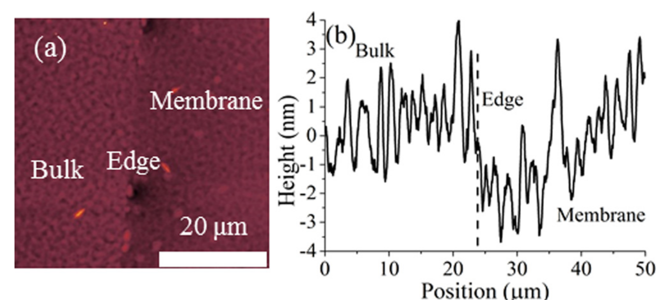

FIG. 5. AFM surface scans showing (a) the surface morphology and (b) the extracted height profiles across the membrane edge.

This article is copyrighted as indicated in the article. Reuse of AIP content is subject to the terms at: http://scitation.aip.org/termsconditions. Downloaded to IP: 161.111.180.191 On: Wed, 23 Dec 2015 11:22:53

unlike scanning X-ray micro-diffraction, the strain relaxation and tilt at the edges is not observed with micro-Raman.

To conclude, we report spatially resolved X-ray micro-diffraction across a 114 nm thick suspended Ge membrane. This technique provides a non-contact and non-destructive method for studying the local crystalline quality of single crystal suspended structures. X-ray diffraction was used as the lattice parameter, strain, crystalline quality and tilt can be determined in a single measurement. The membranes are platforms for further epitaxial growth of any semiconductor materials compatible with Ge and if there is significant tilt or bending at the edges of the membranes incorporating the membranes into devices is problematic. Raman measurements may be able to provide a two-dimensional strain map of the membranes; however, if the layer is tilted this information can become distorted and no information on crystallographic parameters such as tilt can be determined. The membranes have the potential to be excellent growth and integration platforms: compared to bulk Ge epitaxially grown on Si (001) they are perfectly flat and XRD and PV-TEM confirm the misfit dislocation network has been removed. Preliminary strain analysis shows that the strain profile across the membrane is symmetrical and the membrane is slightly more tensile strained than the bulk material. The strain variation across the membrane is sufficiently small that optical device performance would not be affected by strain-induced variation in the Ge bandgap across the entire membrane.[23] Coupled with the smoother surface and absence of misfit dislocation network, compared to the bulk material, we have shown that these tensile strained Ge membranes are excellent strain tuning platforms for optical applications.

This work was carried out under the RCUK Basic Technology Programme supported by research Grant Nos. EP/F040784/1, EP/J001074/1, EP/L007010/1, by the European Community's Seventh Framework Programme (FP7/2007-2013) under Grant Agreement NANOFUNCTION No. 257375, by TAPHOR (MAT2012–31392), and by FP7 project MERGING (Grant No. 309150). This research used equipment funded by AWM and ERDF through the Science City Energy Efficiency project. The Diamond Light Source is acknowledged for providing beamtime. K. J. S. Sawhney is acknowledged for support and encouragement.

[1]R. Pillarisetty, Nature **479**(7373), 324 (2011).
[2]C. Shen, T. Trypiniotis, K. Y. Lee, S. N. Holmes, R. Mansell, M. Husain, V. Shah, X. V. Li, H. Kurebayashi, I. Farrer, C. H. De Groot, D. R. Leadley, G. Bell, E. H. C. Parker, T. Whall, D. A. Ritchie, and C. H. W. Barnes, Appl. Phys. Lett. **97**(16), 162104 (2010).
[3]J. Michel, J. Liu, and L. C. Kimerling, Nat. Photonics **4**(8), 527 (2010).
[4]J. Liu, X. Sun, R. Camacho-Aguilera, L. C. Kimerling, and J. Michel, Opt. Lett. **35**(5), 679 (2010).
[5]V. A. Shah, A. Dobbie, M. Myronov, D. J. F. Fulgoni, L. J. Nash, and D. R. Leadley, Appl. Phys. Lett. **93**(19), 192103 (2008).
[6]V. A. Shah, A. Dobbie, M. Myronov, and D. R. Leadley, Thin Solid Films **520**(8), 3227 (2012).
[7]V. A. Shah, A. Dobbie, M. Myronov, and D. R. Leadley, Thin Solid Films **519**(22), 7911 (2011).
[8]J. M. Hartmann, A. Abbadie, A. M. Papon, P. Holliger, G. Rolland, T. Billon, J. M. Fédéli, M. Rouvière, L. Vivien, and S. Laval, J. Appl. Phys. **95**(10), 5905 (2004).
[9]H.-C. Luan, D. R. Lim, K. K. Lee, K. M. Chen, J. G. Sandland, K. Wada, and L. C. Kimerling, Appl. Phys. Lett. **75**(19), 2909 (1999).
[10]J. Hess, J. Schreiber, S. Hildebrandt, and R. Labusch, Phys. Status Solidi B **172**(1), 225 (1992).
[11]S. A. Shevchenko, J. Exp. Theor. Phys. **88**(1), 66 (1999).
[12]T. A. Langdo, M. T. Currie, Z. Y. Cheng, J. G. Fiorenza, M. Erdtmann, G. Braithwaite, C. W. Leitz, C. J. Vineis, J. A. Carlin, A. Lochtefeld, M. T. Bulsara, I. Lauer, D. A. Antoniadis, and M. Somerville, Solid-State Electron. **48**(8), 1357 (2004).
[13]V. A. Shah, M. Myronov, C. Wongwanitwatana, L. Bawden, M. J. Prest, J. S. Richardson-Bullock, S. Rhead, E. H. C. Parker, T. E. Whall, and D. R. Leadley, Sci. Technol. Adv. Mater. **13**(5), 055002 (2012).
[14]J. R. Haynes and W. Shockley, Phys. Rev. **75**(4), 691 (1949).
[15]G. K. Teal, IEEE Trans. Electron Devices **23**(7), 621 (1976).
[16]H. R. Huff, AIP Conf. Proc. **683**(1), 3 (2003).
[17]T. Tritt, *Thermal Conductivity: Theory, Properties and Applications* (Springer, Clemson, South Carolina, 2004).
[18]B. Bhushan, *Handbook of Nanotechnology* (Springer, 2007).
[19]W. O. Davis, R. Sprague, J. Miller, and IEEE, *MEMS-Based Pico Projector Display* (IEEE, New York, 2008).
[20]G. Rempe, R. J. Thompson, H. J. Kimble, and R. Lalezari, Opt. Lett. **17**(5), 363 (1992).
[21]J. M. Bustillo, R. T. Howe, and R. S. Muller, Proc. IEEE **86**(8), 1552 (1998).
[22]D. Nam, D. Sukhdeo, S.-L. Cheng, A. Roy, K. Chih-Yao Huang, M. Brongersma, Y. Nishi, and K. Saraswat, Appl. Phys. Lett. **100**(13), 131112 (2012).
[23]D. Nam, D. Sukhdeo, A. Roy, K. Balram, S. L. Cheng, K. C. Y. Huang, Z. Yuan, M. Brongersma, Y. Nishi, D. Miller, and K. Saraswat, Opt. Express **19**(27), 25866 (2011).
[24]M. El Kurdi, H. Bertin, E. Martincic, M. de Kersauson, G. Fishman, S. Sauvage, A. Bosseboeuf, and P. Boucaud, Appl. Phys. Lett. **96**(4), 041909 (2010).
[25]F. Bianco, K. Fedus, F. Enrichi, R. Pierobon, M. Cazzanelli, M. Ghulinyan, G. Pucker, and L. Pavesi, Semicond. Sci. Technol. **27**(8), 085009 (2012).
[26]F. Ferrieu, P. Ribot, and J. L. Regolini, Thin Solid Films **373**(1–2), 211–215 (2000).
[27]J. Stangl, C. Mocuta, A. Diaz, T. H. Metzger, and G. Bauer, ChemPhysChem **10**(17), 2923 (2009).
[28]C. Mocuta, J. Stangl, K. Mundboth, T. H. Metzger, G. Bauer, I. A. Vartanyants, M. Schmidbauer, and T. Boeck, Phys. Rev. B **77**(24), 245425 (2008).
[29]M. Hanke, M. Dubslaff, M. Schmidbauer, T. Boeck, S. Schoder, M. Burghammer, C. Riekel, J. Patommel, and C. G. Schroer, Appl. Phys. Lett. **92**(19), 193109 (2008).
[30]D. Chrastina, G. M. Vanacore, M. Bollani, P. Boye, S. Schoder, M. Burghammer, R. Sordan, G. Isella, M. Zani, and A. Tagliaferri, Nanotechnology **23**(15), 155702 (2012).
[31]C. E. Murray, A. Ying, S. M. Polvino, I. C. Noyan, M. Holt, and J. Maser, J. Appl. Phys. **109**(8), 083543 (2011).
[32]N. Hrauda, J. J. Zhang, E. Wintersberger, T. Etzelstorfer, B. Mandl, J. Stangl, D. Carbone, V. Holy, V. Jovanovic, C. Biasotto, L. K. Nanver, J. Moers, D. Grutzmacher, and G. Bauer, Nano Lett. **11**(7), 2875 (2011).
[33]T. Etzelstorfer, M. J. Suess, G. L. Schiefler, V. L. R. Jacques, D. Carbone, D. Chrastina, G. Isella, R. Spolenak, J. Stangl, H. Sigg, and A. Diaz, J. Synchrotron Radiat. **21**(1), 111 (2014).
[34]O. Tabata, R. Asahi, H. Funabashi, K. Shimaoka and S. Sugiyama, Sens. Actuators, A **34**(1), 51 (1992).
[35]K. J. S. Sawhney, I. P. Dolbnya, M. K. Tiwari, L. Alianelli, S. M. Scott, G. M. Preece, U. K. Pedersen, and R. D. Walton, AIP Conf. Proc. **1234**(1), 387 (2010).
[36]P. Fewster, J. Appl. Crystallogr. **25**(6), 714 (1992).
[37]J. S. Reparaz, A. Bernardi, A. R. Goñi, M. I. Alonso, and M. Garriga, Appl. Phys. Lett. **92**(8), 081909 (2008).

This article is copyrighted as indicated in the article. Reuse of AIP content is subject to the terms at: http://scitation.aip.org/termsconditions. Downloaded to IP: 161.111.180.191 On: Wed, 23 Dec 2015 11:22:53